

Sensitivity of model calculations to uncertain inputs, with an application to neutron star envelopes

R. I. Epstein *Nordita, Blegdamsvej 17, DK-2100 Copenhagen, Denmark*

E. H. Gudmundsson *Nordita, Blegdamsvej 17, DK-2100 Copenhagen, Denmark and Science Institute, University of Iceland, Dunhaga 3, 107 Reykjavik, Iceland*

C. J. Pethick *Nordita, Blegdamsvej 17, DK-2100 Copenhagen, Denmark and Department of Physics, University of Illinois at Urbana-Champaign, 1110 W. Green St, Urbana, Illinois 61801, USA*

Received 1982 October 21; in original form 1982 February 2

Summary. A method is given for determining the sensitivity of certain types of calculations to the uncertainties in the input physics or model parameters; this method is applicable to problems that involve solutions to coupled, ordinary differential equations. In particular the sensitivity of calculations of the thermal structure of neutron star envelopes to uncertainties in the opacity and equation of state is examined. It is found that the uncertainties in the relationship between the surface and interior temperatures of a neutron star are due almost entirely to the imprecision in the values of the conductive opacity in the region where the ions form a liquid; here the conductive opacity is, for the most part, due to the scattering of electrons from ions.

1 Introduction

In the study of complex astrophysical phenomena one is frequently faced with problems that involve extensive calculations for which the basic physical inputs or model parameters are not necessarily well known. The investigator must therefore determine how reliable the results of these calculations are and which aspects of the problem need to be understood better. Many problems of this sort can be formulated in such a way that they involve numerically solving N coupled ordinary differential equations of the form

$$\frac{dy_i}{dx} = h_i(x, \mathbf{y}, \mathbf{f}). \quad (1)$$

Here the h_i are functions of x , $\mathbf{y} = (y_1, y_2 \dots y_N)$ and $\mathbf{f} = (f_1, f_2 \dots f_M)$. Each of the input functions f_k describes some piece of the model or of the input physics; these functions themselves depend on the variables x and \mathbf{y} and their number M is arbitrary.

The N boundary conditions that determine the particular solution of equation (1) can be expressed as

$$\lambda_k[\mathbf{y}(x_k)] = 0. \quad (2)$$

Since the x_k are in general different for different k , mixed boundary conditions are allowed for.

In the literature one finds many examples where it is considered important to determine the sensitivities of a solution of equations of the form of equation (1) to the uncertainties in the input physics. The most common approach to the problem has been for the researchers to isolate what appear to be the significant uncertainties and to introduce some adjustable parameters to represent them. The sensitivity analysis then consists of varying each of these parameters and repeatedly solving the model equations to see how the solutions are affected by each of these variations. The shortcoming of this type of parametric approach is that, though it is in principle perfectly adequate, it is laborious and subjective and therefore does not lend itself to complete, systematic sensitivity analyses.

Below is described how a complete sensitivity analysis can be performed without much more labour than that required to solve the problem in the first place. This procedure allows one to determine how the solutions of equation (1) respond to small variations in each of the input functions over every interval in the relevant strip of $(x-y)$ parameter space. Section 2 first gives a naive, brute force procedure for performing the sensitivity analyses and Section 3 then describes an efficient method for obtaining precise sensitivity functions. In Section 4 these methods are used to analyse the sensitivity of calculated thermal structures of neutron star envelopes to the uncertainties in the input physics. Even though the equations governing variation of the temperature with depth in a neutron star envelope appear simple (in fact only a single ordinary differential equation has to be solved; see equation 20, below) much complex physics is involved, and various research groups have obtained discordant results (e.g., Van Riper & Lamb 1981; Glen & Sutherland 1980; Tsuruta 1979). The sensitivity analysis presented here shows which parts of the input physics are most crucial in this problem and allows the discrepancies in the earlier works to be resolved (see Gudmundsson 1981; Gudmundsson, Pethick & Epstein 1982, 1983; hereinafter these references are referred to as Papers I, II and III, respectively).

2 Brute force sensitivity analysis

The question one wants to answer by performing a sensitivity analysis is: how drastically do the solutions of equation (1) vary when any one of the input functions is changed by a small amount in a small region of parameter space? A straightforward way to determine the sensitivity of some solution $y(x)$ to variations in f_k is to increase f_k by a small amount Δf_k in a small interval of x defined by $x_m - s/2 \leq x \leq x_m + s/2$, to again solve equations (1) and (2) and to calculate the changes in $y(x)$, which we denote by $\Delta y(x)$.^{*} For small values of $s\Delta f_k$, the variation $\Delta y(x)$ will depend linearly on the product $s\Delta f_k$, so that a sensitivity function can be defined by

$$\left\langle \frac{\delta y_i(x)}{\delta f_k(x_m)} \right\rangle_\lambda \equiv \frac{\Delta y_i(x)}{s\Delta f_k}. \quad (3)$$

The notation in equation (3) is chosen because for small Δf_k and small s the sensitivity function reduces to the functional derivative. The brackets signify that the right-hand side of the equation only approximates the quantity in the brackets, because finite differences

^{*} The convention used throughout will be that the unperturbed input functions are written as $\mathbf{f} = (f_1, f_2 \dots)$ and the unperturbed solutions to equation (1) with boundary conditions given by equation (2) are written as $\mathbf{y} = (y_1, y_2 \dots)$. Perturbed quantities are given hats, $\hat{\mathbf{f}} = (\hat{f}_1, \hat{f}_2 \dots)$ and $\hat{\mathbf{y}} = (\hat{y}_1, \hat{y}_2 \dots)$ and the differences are expressed as $\Delta \mathbf{y} = (\Delta y_1, \Delta y_2 \dots)$ where $\Delta y_k = \hat{y}_k - y_k$, etc.

are used. The subscript λ indicates that the boundary conditions $\lambda_k = 0$ are satisfied for the perturbed solutions.

The functional derivative $[\delta y_i(x)/\delta f_k(x')]_{\lambda}$ gives precisely the sensitivity information that one wants: the variation in the solutions due to changes in the input functions over a limited portion of parameter space. For example, if $\Delta f_k(x')$ is an arbitrary, but small, variation in one of the input functions $f_k(x')$, then the corresponding variation in the variable y_i is

$$\Delta y_i(x) = \int_{x_a}^{x_b} \left[\frac{\delta y_i(x)}{\delta f_k(x')} \right]_{\lambda} \Delta f_k(x') dx' \quad (3a)$$

where x_a and x_b are, respectively, the lower and upper limits of the interval over which equation (1) is to be solved.

The application of equation (3) to find the sensitivity function, however, can be cumbersome and inefficient. For example, given M input functions (where M can in principle be much larger than the number of coupled equations N) and an x -interval which is divided into S segments, a sensitivity analysis requires $M \times S$ separate solutions to equations (1) and (2). The next section describes how all the possible sensitivity functions for all values of x can be accurately determined with only N additional integrations of equations (1) and (2).

3 Better determinations of the sensitivity functions

The ultimate aim of this section is to find a computationally efficient procedure for obtaining the sensitivity functions for the variations of each of the $y_i(x)$ due to changes in each of the f_k such that *all of the boundary conditions are satisfied*. It is convenient, however, to begin with a somewhat simpler variational problem and then use the solution of this simpler problem to find the sensitivity functions.

Assume that there is a solution $\mathbf{y}(x)$ that satisfies the unperturbed equations (1) and (2). Now allow a perturbation of one f_j in equation (1) such that

$$\begin{aligned} \hat{f}_j(x, y) &= f_j(x, y) + \Delta f_j, & x' < x \leq x' + s \\ &= f_j(x, y), & \text{otherwise.} \end{aligned} \quad (4)$$

The boundary conditions for the required perturbed solution $\hat{\mathbf{y}}(x)$ are specified by setting $\hat{\mathbf{y}}$ equal to \mathbf{y} for $x \leq x'$; this is an allowed solution since $\hat{f} = f$ for $x \leq x'$. The perturbed solution thus satisfies all the boundary conditions for which $x_k < x'$ in equation (2) but not necessarily those for $x_k > x'$. For small values of $s\Delta f_j$ the difference between the original and the new solution can be expressed as

$$\hat{y}_i(x) - y_i(x) = \left[\frac{\delta y_i(x)}{\delta f_j(x')} \right]_{(x' -)} s\Delta f_j. \quad (5)$$

The subscript $(x' -)$ indicates that $\hat{\mathbf{y}}$ is constrained for $x < x'$.

In the Appendix it is shown that the functional derivative in equation (5) is given by

$$\left[\frac{\delta y_i(x)}{\delta f_j(x')} \right]_{(x' -)} = \sum_{k=1}^N \left(\frac{\partial h_k}{\partial f_j} \right)_{x', y(x')} \left[\frac{\partial y_i(x)}{\partial y_k(x')} \right]_{f, y_m \neq k} \theta(x - x'). \quad (6)$$

Here the partial derivative $\partial h_k/\partial f_j$ is evaluated at point x' with the unperturbed values of $y(x')$, the next factor gives the response of $y_i(x)$ to a change of y_k at point x' , and θ is a

step function which incorporates the constraint that $\mathbf{y}(x)$ is unperturbed for $x < x'$. The subscript \mathbf{f} denotes that $\mathbf{f}(x, \mathbf{y})$ is everywhere unperturbed, and the subscript $y_m \neq k$ indicates that all the $y_m(x')$ are held constant except for $y_k(x')$.

The sensitivity functions can be related to the constrained functional derivative (equation 6), if one considers the solutions $\mathbf{y}(x)$ to be functionals of the $f_k(x)$ and functions of the $\lambda_m(x_m)$ of equation (2) which are now allowed to be non-zero; that is $\mathbf{y} = \mathbf{y}(x, \mathbf{f}, \boldsymbol{\lambda})$. For $x > x'$ chain rule functional differentiation yields

$$\left[\frac{\delta y_i(x)}{\delta f_k(x')} \right]_{(x' -)} = \left[\frac{\delta y_i(x)}{\delta f_k(x')} \right]_{\boldsymbol{\lambda}} + \sum_{m=1}^N \left[\frac{\partial y_i(x)}{\partial \lambda_m} \right]_{\mathbf{f}, \lambda_j \neq m} \left[\frac{\delta \lambda_m}{\delta f_k(x')} \right]_{(x' -)} \quad (7)$$

Here the subscript $\boldsymbol{\lambda}$ indicates that all the λ_k are zero and the subscript $\lambda_j \neq m$ indicates that all the λ_j are zero except for λ_m .

Because each boundary function, λ_m , is a function of only the respective $\mathbf{y}(x_m)$ one has

$$\left[\frac{\delta \lambda_m}{\delta f_k(x')} \right]_{(x' -)} = \sum_{n=1}^N \left[\frac{\partial \lambda_m}{\partial y_n(x_m)} \right]_{y_l \neq n} \left[\frac{\delta y_n(x_m)}{\delta f_k(x')} \right]_{(x' -)} \quad (8)$$

For $x < x'$ one can obtain the counterparts of the above expressions which involve $[\delta y_i(x)/\delta f_k(x')]_{(x'+)}$; this is the constrained variational derivative such that $\hat{y}(x)$ is unperturbed for $x > x'$; it is given by an analogous equation to equation (6) with $\theta(x - x')$ replaced by $\theta(x' - x)$.

Putting equations (6), (7) and (8) and their counterparts together one arrives at a general expression for the sensitivity function

$$\begin{aligned} \left[\frac{\delta y_i(x)}{\delta f_j(x')} \right]_{\boldsymbol{\lambda}} = & \sum_{m=1}^N \left(\frac{\partial h_m}{\partial f_j} \right)_{x', \mathbf{y}(x')} \left\{ \left[\frac{\partial y_i(x)}{\partial y_m(x')} \right]_{\mathbf{f}, y_j \neq m} - \sum_{n=1}^N \sum_{k=1}^N \left[\frac{\partial y_n(x_k)}{\partial y_m(x')} \right]_{\mathbf{f}, y_l \neq m} \right. \\ & \left. \times \left[\frac{\partial \lambda_k}{\partial y_n(x_k)} \right]_{y_h \neq n} \left[\frac{\partial y_i(x)}{\partial \lambda_k} \right]_{\mathbf{f}, \lambda_l \neq k} H_k(x, x') \right\} \quad (9) \end{aligned}$$

where

$$H_k(x, x') = \theta(x' - x)\theta(x_k - x) + \theta(x - x')\theta(x - x_k). \quad (10)$$

The great convenience of this expression for the sensitivity function is that it only involves the partial derivatives of h_m and λ_k , which are easily found, and the partial derivatives of the form $\partial y_i(x)/\partial \lambda_k$ and $\partial y_i(x)/\partial y_j(x')$ which one can obtain with N additional solutions of the original differential equations with slightly perturbed conditions. To obtain these latter functions one first calculates $\mathbf{y}(x)$, the unperturbed solution to equations (1) and (2). Then, one calculates N additional solutions to equation (1), $\hat{y}_{il}(x)$, $l = 1 \dots N$ by, in turn, setting only one of the λ_l equal to some small non-zero value, say $\Delta\lambda_l$. For sufficiently small $\Delta\lambda_l$ we have

$$\left[\frac{\partial y_i(x)}{\partial \lambda_l} \right]_{\lambda_j \neq l} = \frac{\hat{y}_{il}(x) - y_i(x)}{\Delta\lambda_l} \quad (11)$$

To obtain the partial derivatives $[\partial y_i(x)/\partial y_k(x')]_{\mathbf{f}, y_j \neq k}$ one uses the already computed $N + 1$ solutions to construct the matrices

$$\Delta Y_{il}(x) \equiv \hat{y}_{il}(x) - y_i(x) \quad (12)$$

at each value of x . For small perturbations a Taylor series expansion gives

$$\Delta Y_{il}(x) = \sum_{j=1}^N \left[\frac{\partial y_i(x)}{\partial y_j(x')} \right]_{f, y_m \neq j} \Delta Y_{jl}(x') \quad (13)$$

which can be inverted to give

$$\left[\frac{\partial y_i(x)}{\partial y_j(x')} \right]_{f, y_m \neq j} = \sum_{l=1}^N \Delta Y_{il}(x) \Delta Y_{lj}^{-1}(x') \quad (14)$$

where $\Delta Y_{lj}^{-1}(x')$ are the elements of the inverse of $\Delta Y_{il}(x')$ such that

$$\sum_{l=1}^N \Delta Y_{kl}(x') \Delta Y_{lj}^{-1}(x') = \delta_{jk} \quad (15)$$

where δ_{jk} is the Kronecker delta function.

4 Neutron star envelopes

The most significant temperature gradients in a hot neutron star occur in the relatively thin layer of the neutron star envelope, the region which extends from the surface to densities of the order $10^{10} \text{ g cm}^{-3}$. At greater densities the star tends to be isothermal, except for a redshift factor. To relate the observable temperature of neutron star surfaces with the interior conditions one needs a relationship between T_s and the temperature T_b at the inner boundary of the envelope. In this study the inner boundary is defined to be at a density $\rho_b = 10^{10} \text{ g cm}^{-3}$.

For a neutron star which has no magnetic field and is more than a few tens of years old, the two equations to be solved are (see Papers I or III) the equation of hydrostatic equilibrium

$$\frac{dP}{dz} = \rho g_s, \quad (16)$$

and the thermal transport equation

$$\frac{dT}{dz} = \frac{3}{16} \kappa \rho \frac{T_s^4}{T^3}. \quad (17)$$

Here P is the pressure, z is a coordinate measuring the distance from the surface of the star, g_s is the surface gravity of the star (as measured by a local observer), ρ is the mass–energy density, T is the temperature, T_s the effective surface temperature and κ is the opacity.

Eliminating the spatial variable z from equations (16) and (17) one finds

$$\frac{d \ln T}{d \ln \rho} = \frac{3}{16} \frac{\kappa \rho}{g_s} \left(\frac{T_s}{T} \right)^4 \left(\frac{dP}{d\rho} \right)_{T(\rho)}. \quad (18)$$

It is convenient to work with logarithmic quantities here since the variables span many decades. The derivative of P with respect to ρ is for changes along a given $T(\rho)$ profile. This derivative can be expanded as

$$\left(\frac{dP}{d\rho} \right)_{T(\rho)} = \left(\frac{\partial P}{\partial \rho} \right)_T + \left(\frac{\partial P}{\partial T} \right)_\rho \frac{dT}{d\rho}. \quad (19)$$

Inserting equation (19) into (18) one finds

$$\frac{d \ln T}{d \ln \rho} = \frac{3}{16} \frac{\kappa}{g_s} \left(\frac{T_s}{T} \right)^4 P'_\rho \left[1 - \frac{3}{16} \frac{\kappa}{g_s} \left(\frac{T_s}{T} \right)^4 P'_T \right]^{-1} \quad (20)$$

where

$$P'_\rho \equiv \left(\frac{\partial P}{\partial \ln \rho} \right)_T \quad (21a)$$

and

$$P'_T \equiv \left(\frac{\partial P}{\partial \ln T} \right)_\rho. \quad (21b)$$

As discussed in Papers I and III, equation (20) is accurate to better than $R_G h_E / R^2$, where R_G is the Schwarzschild radius of the star, h_E is the thickness of the envelope and R is the stellar radius. The quantity $R_G h_E / R^2$ is very insensitive to the mass and radius of the neutron star, and for $\rho_b = 10^{10} \text{ g cm}^{-3}$ it has a value $\approx 5 \times 10^{-3}$.

Equation (20) contains only one parameter that depends on the neutron star model; this is T_s^4 / g_s . There are three factors which describe different aspects of the input physics: the opacity, κ ; the pressure–density factor, P'_ρ ; and the pressure–temperature factor, P'_T . The aim of studying neutron star envelopes is to determine the T_b versus T_s relation for various choices of the model parameter and to understand how sensitive the derived relation is to the uncertainties in the three input physics functions. The T_b versus T_s relation is discussed in Papers I, II and III. Here we will concentrate on the sensitivity analysis. We proceed by first focusing on the sensitivity functions and then by examining the physics that goes into

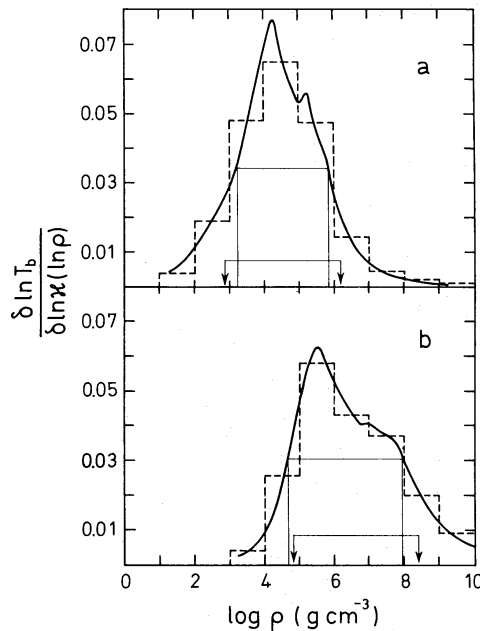


Figure 1. The values of differential sensitivity functions for opacity variations for two values of T_s^4/g_s : (a) $10^8 \text{ K}^4 \text{ cm}^{-1} \text{ s}^2$ and (b) $10^{10} \text{ K}^4 \text{ cm}^{-1} \text{ s}^2$. The histograms were obtained from equation (3) and the smooth curves from equation (22). The thin-lined rectangles indicate the half-maximum sensitive region and the arrows give the sensitive regions defined by where the integral sensitivity function (Fig. 4) is between 10 and 90 per cent of the maximum value.

the equation of state and the opacity and how large the uncertainties in these input functions are.

As a first illustration of a sensitivity analysis, the simple brute force technique is used to obtain the sensitivity function for variations in the opacity. Equation (20) was solved with the 'best estimate' or unperturbed values for κ ; the value of κ was then increased by 10 per cent over a range of one decade in density and a new solution to the thermal structure was found. Many similar perturbations were made and equation (20) solved again for each of these. The approximate sensitivity function $\langle \delta \ln T_b / \delta \ln \kappa (\ln \rho) \rangle_\lambda$ was then evaluated from equation (3). The histograms in Fig. 1 show the results of these efforts for two envelope models; $T_s^4/g_s = 10^8$ and $10^{10} \text{ K}^4 \text{ s}^2 \text{ cm}^{-1}$.

Now consider the method of Section 3 for finding the sensitivity functions. The set of equations (1) for the problem is the single equation (20), so the sensitivity function, equation (9), simplifies in this case to

$$\left[\frac{\delta \ln T_b}{\delta f_j(\rho)} \right]_{T_s} = \left(\frac{\partial h}{\partial f_j} \right)_{\rho, T(\rho)} \left[\frac{\partial \ln T_b}{\partial \ln T(\rho)} \right]_f, \quad (22)$$

where h is the right-hand side of equation (20) and the f_j are $\ln \kappa$, $\ln P'_\rho$ and $\ln P'_T$. The second term on the right-hand side of equation (9) vanishes because the boundary condition, $T - T_s = 0$, is imposed at the surface of the star. The derivatives $\partial h / \partial f_j$ are

$$\frac{\partial h}{\partial \ln \kappa} = h \left(1 + \frac{P'_T}{P'_\rho} h \right), \quad (23)$$

$$\frac{\partial h}{\partial \ln(P'_\rho)} = h \quad (24)$$

and

$$\frac{\partial h}{\partial \ln(P'_T)} = \frac{P'_T}{P'_\rho} h^2. \quad (25)$$

By performing two integrations of equation (20), one with surface temperature T_s and one with a slightly raised surface temperature, one can evaluate $\partial \ln T_b / \delta \ln T$. (The model parameter T_s^4/g_s must be the same for both integrations.) The complete set of sensitivity functions for variations in the opacity and for variations in the equation of state factors then follows from equation (22); these are shown by the smooth curves in Figs (1) and (2). Equations (23)–(25) show that the three sensitivity functions are related by

$$\frac{\delta \ln T_b}{\delta \ln \kappa (\ln \rho)} = \frac{\delta \ln T_b}{\delta \ln P'_\rho (\ln \rho)} + \frac{\delta \ln T_b}{\delta \ln P'_T (\ln \rho)}. \quad (26)$$

Fig. 1 shows that the results of the brute force method and the present method are in essential agreement; however, one obtains more information using the method of Section 3 than is obtained with many separate numerical integrations using the brute force technique.

We can now turn to the interpretation of the results of this sensitivity analysis. First it should be noted that the sensitivity function falls off at very low densities and at very high densities. This could have been expected for the following reasons: Near the surface of a neutron star, the thermal structure tends to converge to the radiative-zero solution (Schwarzschild 1958). Therefore, perturbations in the opacity or equation of state at low densities are effectively 'forgotten'. At the other end, at high densities, the envelope

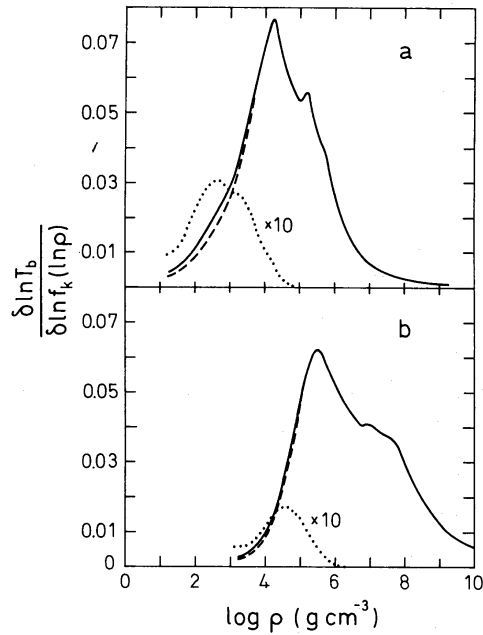


Figure 2. The sensitivity functions for variations in the opacity (solid line) and variations in the equation of state factor P'_ρ (dashed line) and P'_T (dotted line). The neutron star envelope parameters are (a) $10^8 \text{ K}^4 \text{ cm}^{-1} \text{ s}^2$ and (b) $10^{10} \text{ K}^4 \text{ cm}^{-1} \text{ s}^2$.

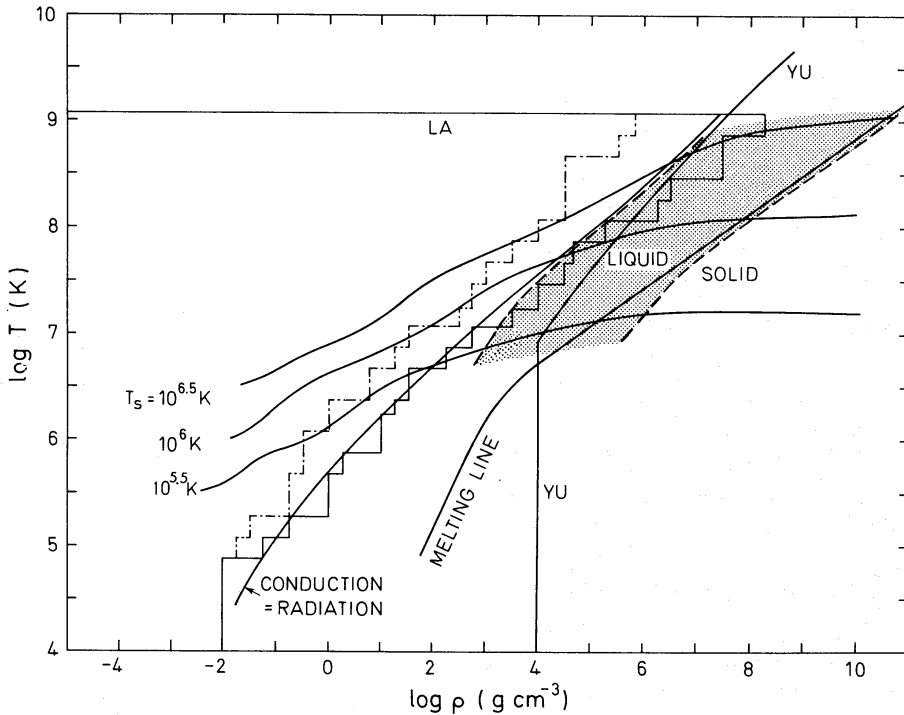


Figure 3. Sources of opacity. Above the line marked 'conduction = radiation' heat is transported primarily by radiative diffusion, and below it by thermal conduction. The ions crystallize below the melting line. Within the step-line boundaries we use the Los Alamos (LA) radiative (continuous line) and conductive (dash-dot line) opacities (Huebner *et al.* 1977). Below the line marked YU the conductive opacities derived by Yakovlev & Urpin (1980) and Urpin & Yakovlev (1980) are used. Several temperature profiles are shown for neutron stars with surface gravities $g_s = 10^{14} \text{ cm s}^{-2}$ and effective surface temperatures $T_s = 10^{5.5}$, 10^6 and $10^{6.5} \text{ K}$. The shaded area indicates the sensitive region in which the opacity needs to be accurately determined.

becomes nearly isothermal. In this region it again does not matter if there are uncertainties in the input physics, as long as they are not so large as to greatly disturb the isothermality.

To see which parts of the input physics are important, we have defined a sensitive region in the ρ - T plane, as that region for which $\delta \ln T_b / \delta \ln \kappa (\ln \rho)$ is greater than 1/2 of its maximum value for each temperature contour. Sensitive regions for the equation of state factors may be defined in a similar way, but we shall not describe them in detail, since the equation of state is known much better than the opacity (see below). This region is indicated by the grey area in Fig. 3. To obtain reliable values of T_b , one should concentrate on understanding the opacity and equation of state in this limited region.

It should be mentioned that there is some ambiguity inherent in the definition of the sensitive region. The exact boundaries of the sensitive region depend on our choice of $\ln \rho$ as the independent variable. If we had chosen ρ instead, we would have obtained a somewhat different sensitive region. This ambiguity is removed when one uses the integral sensitivity function

$$S[y_i(x), f_k; x'] \equiv \int_{x_a}^{x'} \frac{\delta y_i(x)}{\delta \ln f_k(x'')} dx'' \quad (27)$$

The integral sensitivity function gives the variation in the $y_i(x)$ due to small changes in the f_k for *all* x between the lower limit x_a and x' .

In the present case, we are interested in

$$S(T_b, \kappa; \rho) = \int_{v(\rho_a)}^{v(\rho)} \left(\frac{\delta \ln T_b}{\delta \ln \kappa(v)} \right) dv \quad (28)$$

where $v(\rho)$ is an arbitrary monotonic function of the density; the values of $S(T_b, \kappa; \rho)$ do not depend on which function of $v(\rho)$ is used for the independent variable. The integral sensitivity functions corresponding to the smooth curves in Fig. 1 are shown in Fig. 4. In terms of these functions, the sensitive region can be defined as that for which S lies between, say, 10 and 90 per cent of its maximum value. This choice would give the sensitivity bounds indicated by the arrows in Fig. 1. One can see that for the neutron star envelope problem the two methods for determining the sensitive region are in good agreement. This is because in this case the differential sensitivity function is appreciable only over a limited density range. In general, however, it is preferable to use the $S[y_i(x), f_k; x']$ functions rather than the $\delta y_i(x) / \delta f_k(x')$ functions for determining the sensitive regions.

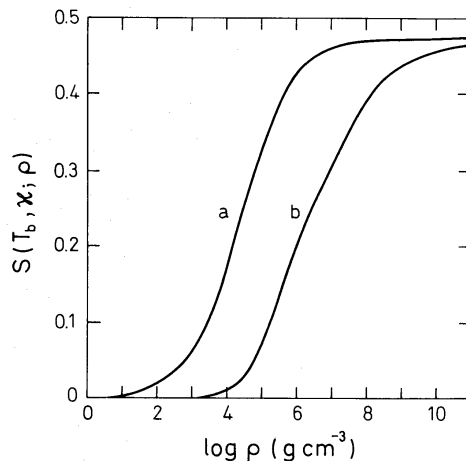


Figure 4. The integral sensitivity function for the differential sensitivity functions shown in Fig. 1.

If κ is everywhere multiplied by a factor α , such that $|1 - \alpha| \ll 1$, then the corresponding change in $\ln T_b$ is given by $S(T_b, \kappa; \rho_b) \ln \alpha$. Our studies of neutron star envelopes (Papers I, II, III) showed that $T_b \propto \alpha^{0.46}$ and thus $S(T_b, \kappa; \rho_b) = 0.46$, in agreement with the results in Fig. (4) obtained from equation (27).

Now consider what physics goes into the opacity and the equation of state, what the important uncertainties are, and how they can ultimately affect the T_b versus T_s relationship. (See Papers I, II, III for a full explanation of the opacity and equation of state, and for a description of what was used for the calculations presented here.)

At low densities, energy is transported mainly by radiation, and the important sources of opacity are bound–bound, bound–free and free–free absorptions. At higher densities, the energy is transported for the most part by thermal conduction. At the lower densities in the conductive region the ions are still in the liquid state, and the conductive opacity is largely due to electron–ion scattering. At higher densities, the ions crystallize and the dominant contributor to the opacity is electron–phonon scattering.

In Fig. 3 the regions in the ρ – T plane where the various processes are most important for determining the net opacity are delineated. Also shown in this figure are the regions for which recent determinations of the opacity exist, and several representative T – ρ profiles for neutron star envelopes. It should be noted that the opacity is a complicated function of the density and the temperature, that the determination of κ in different regions of ρ – T space requires considerations of widely different physics, and finally that accurate values of the opacity are not known everywhere.

Within the sensitivity strip the ions form a liquid, the energy is transported mainly by electron conduction and the most important source of opacity is electron–ion scattering. Two research groups have recently investigated the conductive opacity for these conditions (Flowers & Itoh 1976, FI; Urpin & Yakovlev 1980; Yakovlev & Urpin 1980, referred to collectively as YU). These two groups present opacities which differ by up to a factor of 3 within the sensitivity strip of Fig. 3. Since these are the most frequently referenced results, we take the factor of 3 to be a reasonable estimate for the uncertainty in the opacity functions within the sensitivity strip.

The equation of state for the neutron star envelopes can be accurately represented as the sum of three terms

$$P = P_e + P_i + P_c. \quad (29)$$

Here P_e is the pressure of free electrons, P_i is the pressure of free ions and P_c is the classical Coulomb correction for ion–ion interactions. Corrections due to other factors such as the radiation field, electron–ion and electron–electron Coulomb interactions and quantum effects for the ions are all small for the density–temperature range of importance for most astrophysically relevant neutron star envelopes.

The two main sources of possible error for the equation of state are the uncertainties in the classical Coulomb correction and in the degree of ionization. The Coulomb corrections were estimated from the Monte Carlo calculations of Hansen (1973) and Pollock & Hansen (1973), and should be good to a few per cent. The uncertainties due to partial pressure ionization can be considerably larger than this, especially since the detailed ionization equilibrium calculations of the Los Alamos group do not extend into much of the sensitivity strip. Fortunately the matter in the sensitive region is almost completely ionized for most envelope structures of astrophysical interest. Even at the lowest temperature, lowest density corner of the sensitivity strip in Fig. 3, the matter is at least 80 per cent ionized; elsewhere within the sensitivity strip the degree of ionization is higher. A typical uncertainty in the electron contribution to the equation of state is therefore of the order of 10 per cent; though it could be more for cool neutron stars, especially if T_s is less than 3×10^5 K.

The uncertainties in the value of T_b due to the uncertainties in the opacity and equation of state can be found from equations similar to equation (3a),

$$\Delta \ln T_b \approx \sum_k \int \frac{\delta \ln T_b}{\delta f_k(\ln \rho)} \Delta f_k(\rho) d \ln \rho \quad (30)$$

where $\Delta \ln T_b$ is the uncertainty in $\ln T_b$ and the Δf_k are the uncertainties in the input functions. For rough estimates of the importance of the uncertainties in the opacities and the equation of state, approximate the two largest sensitivity functions $\delta \ln T_b / \delta \ln \kappa$ and $\delta \ln T_b / \delta \ln P'_\rho$ by plateau functions with an amplitude 0.04 and a width of three decades in density. Since the uncertainties in the opacity are of the order of a factor of 3 and the uncertainties in the P'_ρ are of the order of 10 per cent, one finds

$$(\Delta \ln T_b)_\kappa \approx 0.30 \quad (31)$$

$$(\Delta \ln T_b)_{\text{EOS}} \approx 0.03 \quad (32)$$

for the contributions to the uncertainties in the value of T_b due to the possible errors in the opacity and the equation of state, respectively. The possible errors in the equation of state have little effect on the thermal structures considered here and will not be considered further.

To interpret observations it is of most interest to know the surface luminosity for a neutron star of some given internal state. The uncertainties in the value of T_b for a given T_s can be related to the uncertainties in the neutron star luminosity, L , for given T_b by the expression (Papers I, II and III)

$$L \propto T_b^{2.2}. \quad (33)$$

The scaling relation indicates that the opacity uncertainties can lead to errors in the surface luminosity of approximately a factor of 2. This rough estimate agrees with results of our numerical calculations (Paper III).

4 Conclusions

A procedure is given by which one can assess how the uncertainties in the input physics affect the results obtained in the solution of N coupled ordinary differential equations. With only N additional integrations, one can obtain the sensitivity of each of the dependent variables to variations in all of the input functions over the entire relevant region of parameter space.

These results have been applied to the study of the envelopes of neutron stars. It is found that there is a relatively small region of the ρ - T plane for which the opacity must be known very reliably. In this region, the energy is mainly carried by thermal conduction and electron-ion scattering is the dominant source of opacity. The uncertainties in opacity calculations have limited the reliability of the computed luminosities of neutron stars to about a factor of 2.

Acknowledgments

This research was supported in part by NASA grant NSG 7653.

References

- Glen, G. & Sutherland, P. G., 1980. *Astrophys. J.*, **239**, 671.
 Gudmundsson, E. H., 1981. *Licentiate thesis*, University of Copenhagen. (Available as a Nordita Report.)
 Gudmundsson, E. H., Pethick, C. J. & Epstein, R. I., 1982. *Astrophys. J.*, in press.
 Gudmundsson, E. H., Pethick, C. J. & Epstein, R. I., 1983. *Astrophys. J.*, submitted.
 Hansen, J. P., 1973. *Phys. Rev.*, **A8**, 3096.
 Huebner, W. F., Merts, A. L., Magee, N. H. & Argo, M. F., 1977. *Astrophysical Opacity Library, Report No. LA 67607*, Los Alamos Scientific Laboratory.
 Pollock, E. L. & Hansen, J. P., 1973. *Phys. Rev.*, **A8**, 3110.
 Schwarzschild, M., 1958. *Structure and Evolution of the Stars*, Princeton University Press.
 Tsuruta, S., 1979. *Phys. Rept.*, **56**, 237.
 Urpin, V. A. & Yakovlev, D. G., 1980. *Sov. Astr.*, **24**, 126.
 Van Riper, K. A. & Lamb, D. Q., 1981. *Astrophys. J.*, **244**, L13.
 Yakovlev, D. G. & Urpin, V. A., 1980. *Sov. Astr.*, **24**, 303.

Appendix: Calculations of $[\delta y_i(x)/\delta f_k(x')]_{(x' -)}$

The functional derivative $[\delta y_i(x)/\delta f_k(x')]_{(x' -)}$ describes the effects on solutions of equation (1) due to (a) perturbing the input physics functions $f_k(x)$ in a small region about x' and (b) holding the perturbed solution equal to the original solution for $x < x'$.

Let the original solution be $y(x)$ and the perturbed solution be $\hat{y}(x)$. Take the original form of the input physics function to be $f_k(x, y)$ and the perturbed one to be $f_k(x, y) + \Delta f_k$ in the interval x' to $x' + s$. The values of $y_i(x)$ and $\hat{y}_i(x)$ are equal for $x < x'$. Their values at $x + s$ can be obtained from a Taylor series expansion

$$y_i(x' + s) = y_i(x') + h_i s + \dots, \quad (\text{A1})$$

$$\hat{y}_i(x' + s) = y_i(x') + \left(h_i + \frac{\partial h_i}{\partial f_k} \Delta f_k \right) s + \dots \quad (\text{A2})$$

Taking the difference of equations (A1) and (A2) and keeping only lowest order terms, yields

$$\hat{y}_i(x' + s) - y_i(x' + s) = \frac{\partial h_i}{\partial f_k} s \Delta f_k. \quad (\text{A3})$$

In these equations, h_i and $\partial h_i/\partial f_k$ are evaluated at $[x', y(x')]$.

For $x > x' + s$, the solutions $y_i(x)$ and $\hat{y}_i(x)$ obey the same equation but have different boundary conditions at $x' + s$. To express this fact, the dependence of the solutions $y_i(x)$ and $\hat{y}_i(x)$ on the boundary values of the y_j and the \hat{y}_j at $x = x' + s$ is shown explicitly:

$$y_i(x) = y_i[x; x' + s, y_j(x' + s)], \quad (\text{A4})$$

$$\hat{y}_i(x) = y_i[x; x' + s, \hat{y}_j(x' + s)]. \quad (\text{A5})$$

The use of y_i on the right-hand sides of equations (A4) and (A5) expresses the fact that the functional forms are the same in both these equations. Expanding equation (A5) in a Taylor series in $\hat{y}_j - y_j$ and subtracting equation (A4) gives

$$\hat{y}_i(x) - y_i(x) = \sum_{j=1}^N \frac{\partial y_i(x)}{\partial y_j(x' + s)} [\hat{y}_j(x' + s) - y_j(x' + s)], \quad (\text{A6})$$

The functional derivative is given by $[\hat{y}_i(x) - y_i(x)]/s\Delta f_k$ in the limit of small $s\Delta f_k$. Using (A3) and (A6) one obtains for $x > x'$

$$\left[\frac{\delta y_i(x)}{\delta f_k(x')} \right]_{(x' \rightarrow)} = \sum_{j=1}^N \left(\frac{\partial h_j}{\partial f_k} \right)_{x', y(x')} \left[\frac{\partial y_i(x)}{\partial y_j(x')} \right]_{f, y_m \neq j} \quad (\text{A7})$$

The notation used here is the same as in Section 3.

Note added in proof

Recently R. Nandkumar and C. J. Pethick (unpublished) and N. Itoh, S. Mitake, H. Iyetomi & S. Ichimaru (unpublished) have calculated the conductive opacity in the region where the ions are liquid, using improved results for the correlations of the ionic plasma. They find results which are in rather good agreement with the YU ones. We now believe that the conductive opacity is uncertain by much less than the factor 3 quoted in Section 4, and that the uncertainties in the temperature of the inner boundary and the luminosity are correspondingly reduced.